

Supporting Information for

Rational design of a bi-layered reduced graphene oxide film on polystyrene foam for solar-driven interfacial water evaporation

Le Shi, Yuchao Wang, Lianbin Zhang and Peng Wang*

Water Desalination and Reuse Center, Division of Biological and Environmental Sciences and Engineering, King Abdullah University of Science and Technology, Thuwal 23955-6900, Kingdom of Saudi Arabia.

E-mail: peng.wang@kaust.edu.sa

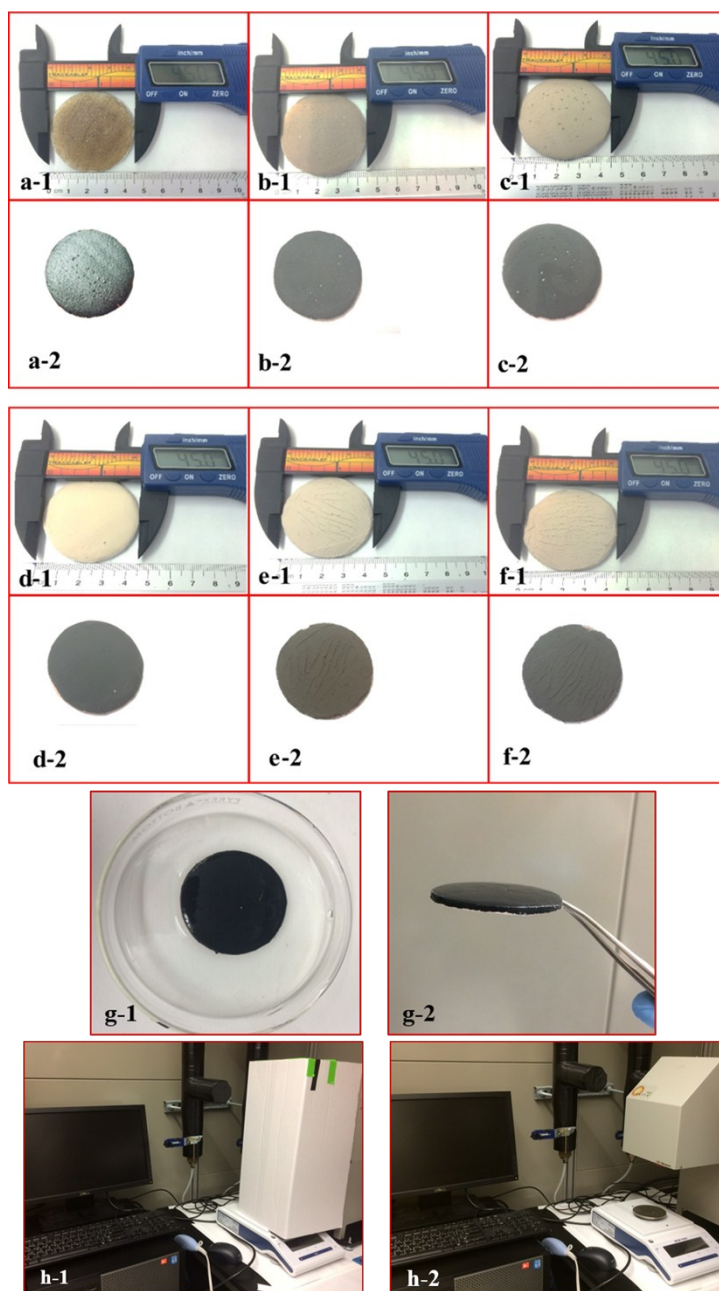


Figure S1 Photographs of the prepared $\text{GSi}_n\text{-PS}$ bi-layered photothermal membranes ($n=0, 0.1, 0.2, 0.3, 0.4$ and 0.5 g) (a1-f1) with diameter of 4.5cm and the same membranes after HI reduction (i.e., $\text{rGSi}_n\text{-PS}$) (a2-f2). Porous $\text{rGSi}_n\text{-PS}$ bi-layered photothermal membrane after SBA-15 removal by NaOH (g1). rGO layer is coated on the peripheral edge (g2). Homemade water evaporation performance measurement system, with white paper as cover (h1), without cover (h2).

There was a significant color change on the membrane surface after GO reduction to rGO. As can be seen, with increasing amount of SBA-15, there were more cracks on the membrane surfaces.

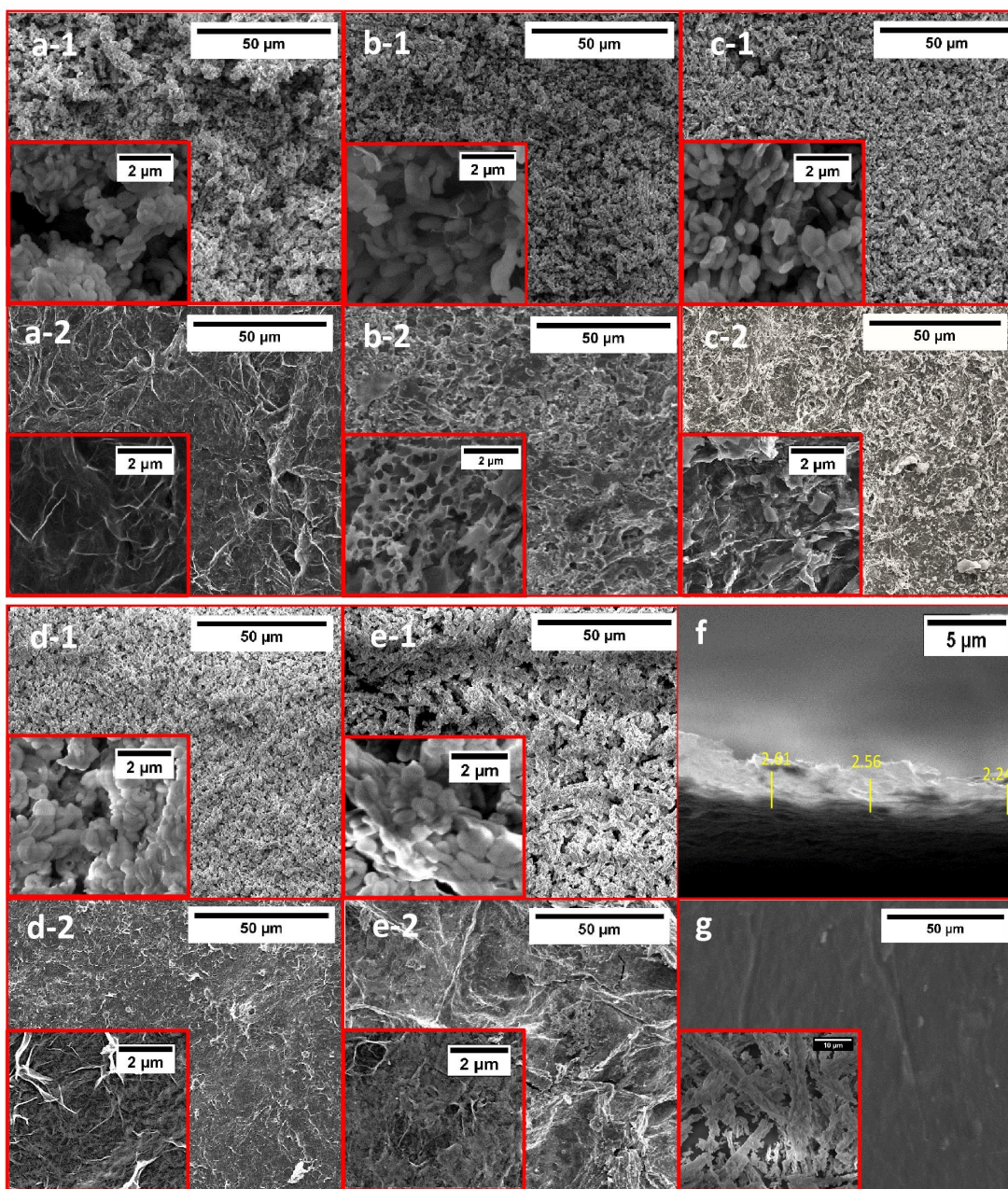


Figure S2 SEM images of the top layer of rGSi_n-PS (n=0, 0.1, 0.2, 0.3, 0.4 and 0.5g) bi-layered photothermal membranes before SBA-15 removal in (a1-e1) respectively, and after SBA-15 removal in (a2-e2) respectively; insets in a-e are magnified views; (f) the cross sectional images of the porous rGSi_{0.2} (i.e., after SBA-15 removal); (g) the top view of the PS substrate.

Figures 2a1-e1 present the rGSi_n-PS bi-layered photothermal membranes. Clearly seen were the bar structure of SBA-15 and the film format of the rGO layer. With increasing amount of SBA-15 powder, there was less rGO that could be seen and more agglomeration happened. The figures 2a2-e2 are the samples after SBA-15 removal, which show porous and 3D network structures of the top layers, with a large amount of inter connected pores (0.5-2.0 μm). The walls of these pores consisted of thin layers of stacked graphene sheets.

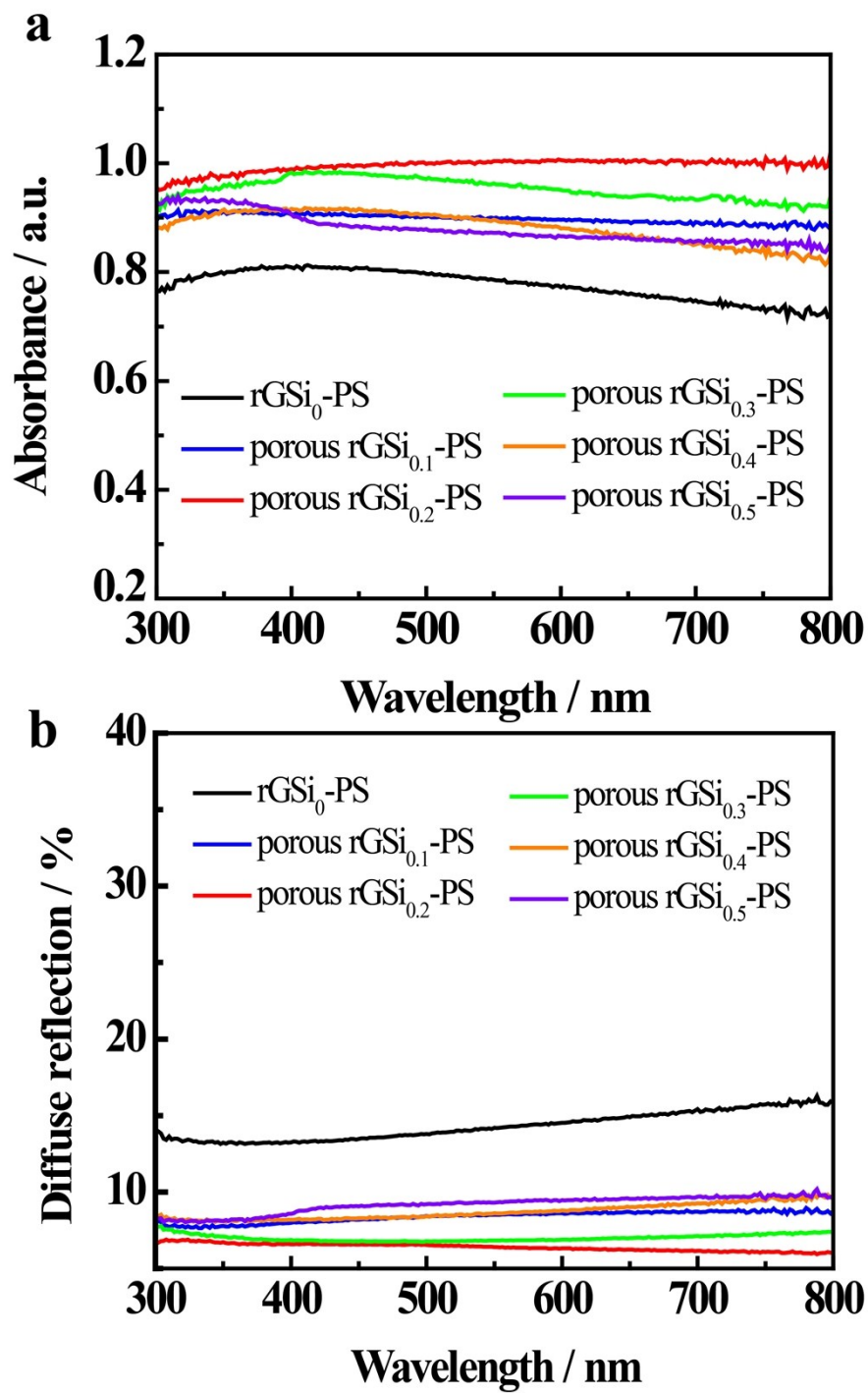


Figure S3 The absorption (a) and diffuse reflection (b) spectra of (porous) rGSi_n-PS, n=0, 0.1, 0.2, 0.3, 0.4, and 0.5 g.

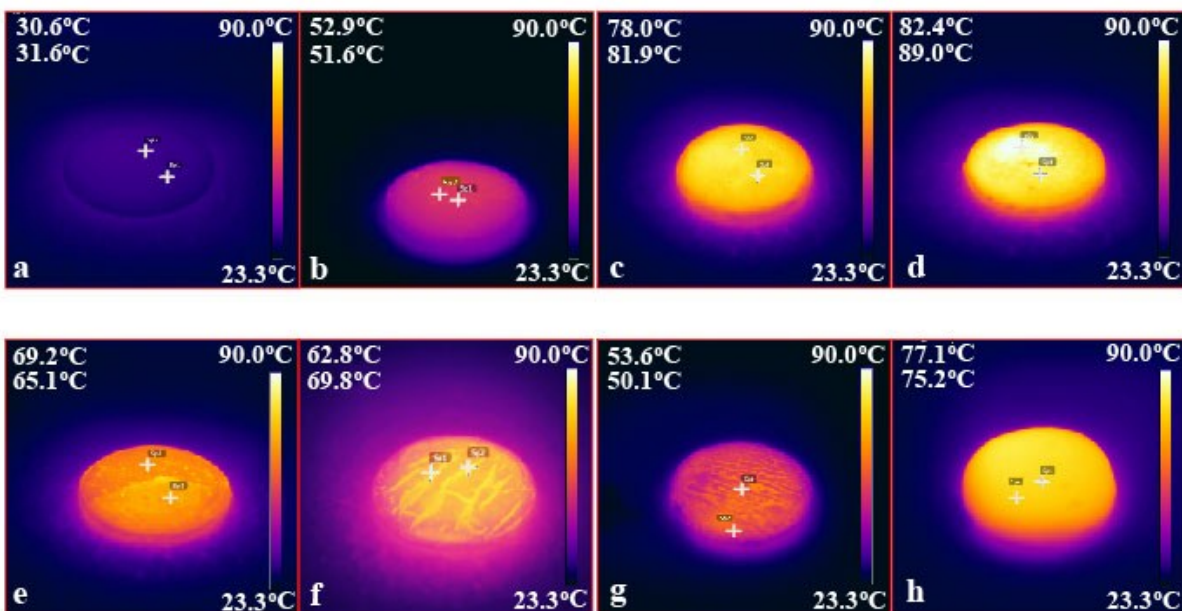


Figure S4 IR images of the (porous) rGSi_n-PS bi-layered photothermal membranes after 100s illumination: PS substrate (a) uncoated, coated (b) with rGSi₀, (c) with porous rGSi_{0.1}, (d) with porous rGSi_{0.2}, (e) with porous rGSi_{0.3}, (f) with porous rGSi_{0.4}, (g) with porous rGSi_{0.5} respectively. As a control experiment, the PS substrate coated with 4.0 ml GO/0.2 mg SBA-15 without SBA-15 removal was in (h) (i.e. rGSi_{0.2}).

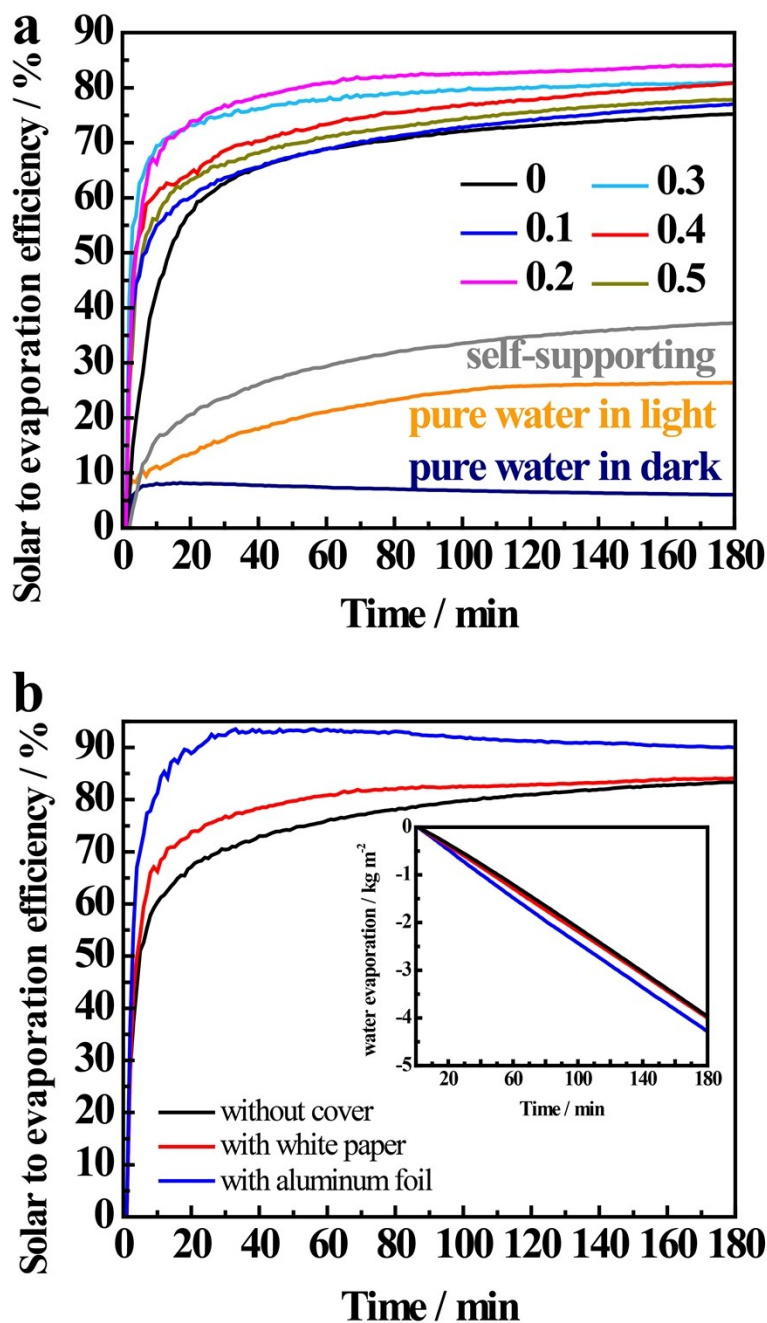


Figure S5 (a) Light to evaporation conversion efficiency of the (porous) rGSi_n-PS bi-layered photothermal membranes prepared with different ratio of GO and SBA-15 (4.0 ml GO with 0, 0.1, 0.2, 0.3, 0.4 and 0.5g SBA-15 respectively), under the otherwise same conditions. As a control experiment, the self-supporting porous rGSi_{0.2} membrane was also tested. (b) Light to evaporation conversion efficiency of rGSi_{0.2}-PS bi-layered photothermal membrane in the different systems with aluminum foil, white paper and

without cover. Inset was the time-course of water evaporation performance of each system.

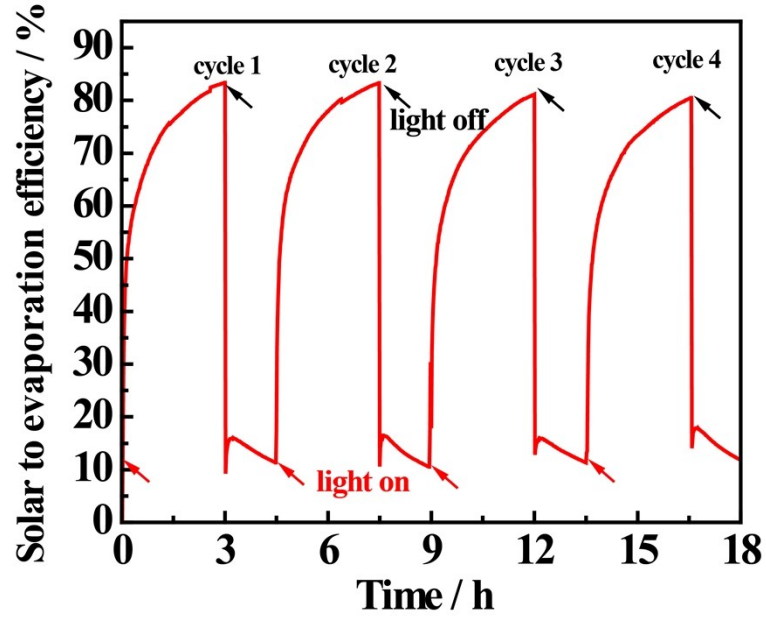


Figure S6 The cycle stability test of the porous rGSi_{0.2}-PS for light to evaporation conversion efficiency for 4 cycles. In each cycle, light is on for 3 hours and light is off for 1.5 hours.

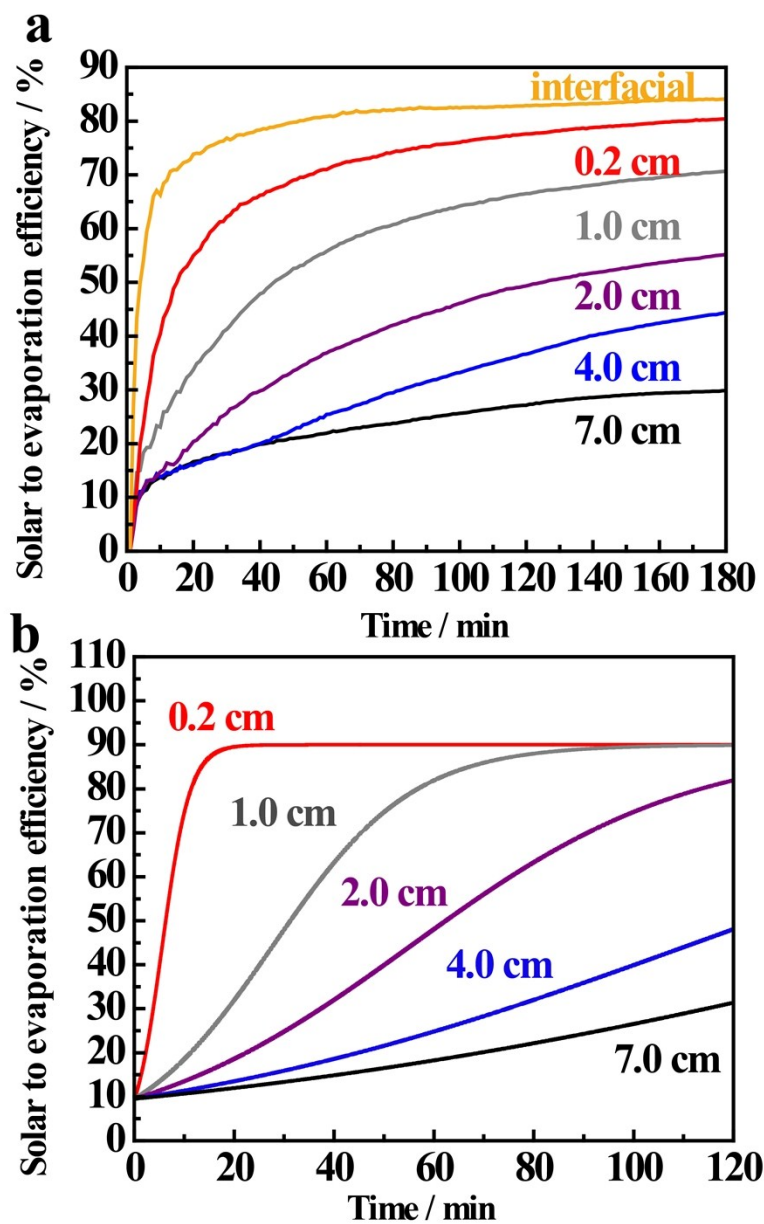


Figure S7. Light to evaporation conversion efficiency of the porous rGSi_{0.2}-PS bi-layered photothermal membranes at different depth under water: (a) experimental efficiency corresponding to the water evaporation performance in Figure 5b and (b) simulated efficiency corresponding to the simulated performance in Figure 5c.

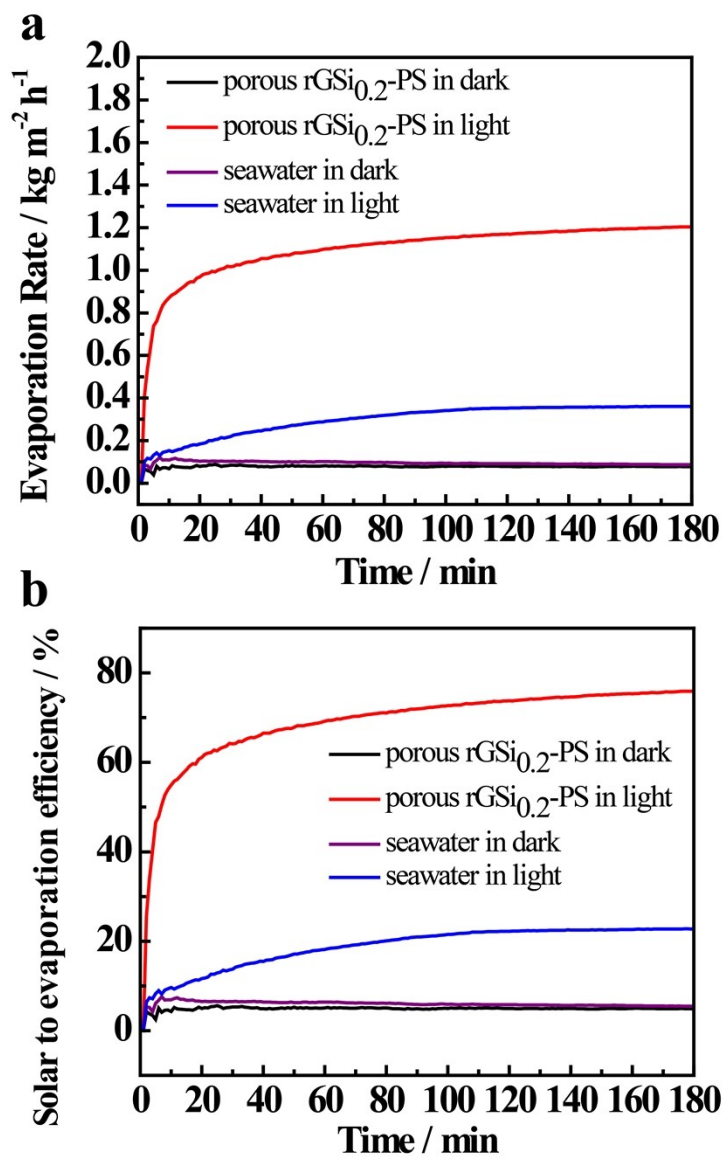


Figure S8. Synthetic seawater evaporation rate and light to evaporation conversion efficiency of the porous rGSi_{0.2}-PS bi-layered photothermal membranes, which was self-floating on the surface of simulated seawater with 3.5% NaCl solution.

Reference	Light intensity (kWm ⁻²)	Photothermal material	Heat barrier material	Evaporation rate	Solar to evaporation efficiency
1	1.0	free floating film of gold nanoparticles	NA	0.4 mg/(s·W)	-
2	10	exfoliated graphite	carbon foam	-	85%
3	1.0	polypyrrole coated stainless steel mesh	NA	-	58%
4	1.0	nitrogen doped porous graphene	NA	-	80%
5	4.5	Au NP	Air laden-paper	-	77.8%
6	3.0	carbon-black-based gauze	NA	6.0g/h	-
7	6.0	aluminium-based plasmonic absorber	NA	-	91%
8	20.0	thin-film black gold membranes	NA	-	57%
9	1.0	carbon nanotube	macroporous silica	-	82%
10	1.0	cermet (BlueTec eta plus) coated copper sheet	Polystyrene foam disk	-	72% at 17°C 28% at 100°C
11	1.0	GO	Polystyrene foam	-	80%
12	1.0	porous rGO	Polystyrene foam	1.31 kg m ⁻² h ⁻¹	83% (this work)

Table S1. The photothermal evaporation performance of a variety of materials reported in the literature, along with the material reported by this work.

Model Simulation

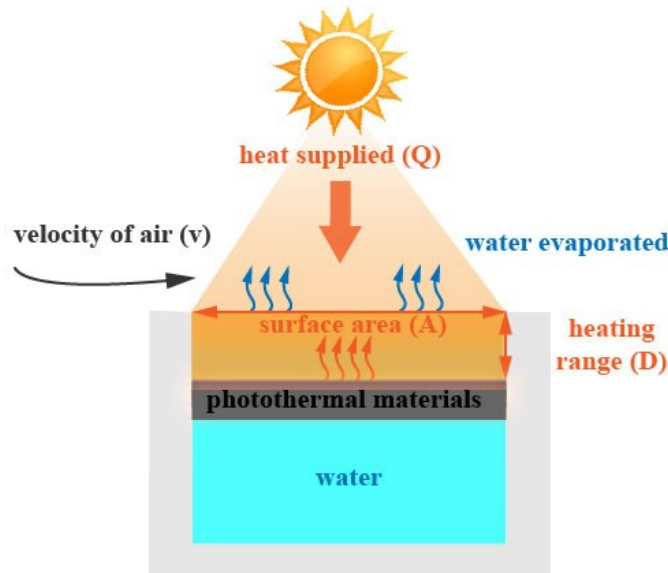


Figure S9. Schematic illustration of the model simulation setup to investigate the relationship between water evaporation performance and heating range (i.e. the thickness of heat water layer on the top of photothermal material). The photothermal material is fixed at different depth under water surface, captures, and converts light to thermal energy (red arrows), which drives water evaporation (blue arrows).

In brief, solar light is shined directly from the top and is captured by photothermal material with a surface area of A , which is placed underwater at a fixed depth. The heating range (D) is the water column directly above the photothermal material. In the model, the driving force to move water molecules from the water surface is the difference between the water vapor pressure at the water surface and that of the bulk air above the water surface and the water vapor, which in turn is dependent on temperature of the air, the surface water, and the movement of air.

To simplify, the models consider the following factors as relevant parameters: water temperature, and temperature, humidity and velocity of the air above the water surface in the model system. The amount of evaporated water is calculated with the following equations:

$$g_s = \theta A(x_s - x)/3600 \quad (\text{S-1})$$

$$\theta = (25 + 19v) \quad (S-2)$$

$$x_s = 0.62198 p_w / (p_a - p_w) \quad (S-3)$$

where g_s is the amount of evaporated water per second (kg/s), θ is evaporation coefficient (kg/m² h), v is the velocity of air above the water surface (m/s), A is the water surface area exposed to solar light (cm²), x_s is humidity ratio of the saturated overlying air (kg/kg) (kg H₂O in kg dry air), and x is humidity ratio of the overlying air (kg/kg) (kg H₂O in kg dry air), p_w is partial pressure of the water vapor in the overlying air (Pa), p_a is atmospheric pressure of the overlying air (Pa). It is worth mentioning that the units of θ in S-1 and S-2 do not match with each other as S-2 is a purely empirical formula. ^{12,13,14}

The maximum amount of water vapor in the air is achieved when $p_w = p_{ws}$ where p_{ws} is saturation pressure of water vapor under the same temperature. p_{ws} varies with the air temperature following S-4:

$$p_{ws} = e^{(77.3450 + 0.0057 T - 7235 / T) / T^{8.2}} \quad (S-4)$$

where e is the constant 2.718 and T is the temperature of the overlying air (K). ¹⁵

At water vapor saturation, x_s is then modified to:

$$x_s = 0.62198 p_{ws} / (p_a - p_{ws}) \quad (S-5)$$

For the simulation: the air temperature was set at 20°C (293K), the relative humidity 60%, the humidity ratio in air 0.0085kg/kg, A 15.89 cm², v above the water surface 0.05 m/s and D ranging between 0.2 and 7.0 cm.

Some of the major simplifying assumptions in the simulation are: (1) a perfect heat barrier is assumed and thus no heat and also light is transported to underlying water column; (2) a uniform temperature profile is assumed for the heating range at all time; (3) a 10% energy loss and thus 90% of the light to evaporation conversion efficiency (i.e., η) of the system is assumed, which is reasonable based on the experimental results in this study.

It is worth pointing out that that thermal radiation accounts for a significant part of energy loss in photothermal water evaporation system and is positively related to the temperature difference between surface water and overlying air, which is then affected by the depth of the photothermal material underwater. However, for the purpose of simplicity, the same energy loss (i.e., 10%) is assumed in the model for all cases.

the water mass in the heating range is calculated as:

$$m = \rho AD = 1.0 \text{ g/cm}^3 AD \quad (\text{S-6})$$

Table 2: weight of water within the different heating range

Distance (cm)	0.2	1.0	2.0	4.0	7.0
Weight (g)	3.178	15.89	31.78	63.56	111.23

D = 0.2 cm is chosen as an exemplifying case here and the simulation results of all the other heating depths can be found in the excel files.

To start the simulation, the amount of the water evaporated at room temperature (with T=293.15K, p_a = 101.325kPa) (i.e., before light illumination) is calculated as follows:

$$p_{ws} = e^{(77.3450 + 0.0057 T - (7235 / T)) / T^{8.2}} = 2318 \text{ (Pa)}$$

$$x_s = 0.62198 p_{ws} / (p_a - p_{ws}) = 0.62198 p_{ws} / (101325 - p_{ws}) = 0.01456 \text{ (kg/kg)}$$

$$g_s = (25 + 19v)A(x_s - x) / 3600$$

$$= (25 + 19 \times 0.05 \text{ m/s}) (2.25 \times 2.25 \times 10^{-4} \times 3.14 \text{ m}^2) \times 0.01456 \text{ kg/kg} \times (1 - 60\%) / 3600$$

$$= 6.67 \times 10^{-8} \text{ kg/s}$$

The energy needed to produce the water evaporation is be calculated as:

$$q = h_{we} g_s \quad (\text{S-7})$$

where q is the heat required (kJ/s, kW), h_{we}=evaporation heat of water (2270kJ/kg).¹⁶ Thus

$$q = 2270 \text{ kJ/kg} \times 6.67 \times 10^{-8} \text{ kg/s} = 0.151 \text{ J/s} = 0.151 \text{ W}$$

In the model, the incoming solar light energy is calculated as:

$$Q = IA \quad (\text{S-8})$$

where Q is the incoming solar energy (W), I is the light intensity of solar simulator (AM1.5 100 W/cm^2). So, $Q = 100 \text{ mW/cm}^2 \times 15.89 \text{ cm}^2 = 1589 \text{ mW} = 1.589 \text{ W}$

With an assumed energy loss of 10%, the energy utilized by water is:

$$P = (1 - 10\%) \times Q = 1.43 \text{ W}$$

In doing the iterative calculation, the temperature of the air above water is set to be equal to the temperature surface water in the first cycle (i.e., the first second in this case) of the simulation (the user has freedom to set cycle interval, such as 1 second, 1 minute, etc.). Thus, the energy available to heat the water within the heating range (q_e) is calculated as:

$$q_e = P - q = 1.43 - 0.151 = 1.279 \text{ W}$$

At the end of this cycle (1 second), the water temperature in the heating range is increased by:

$$dt = \frac{q_e}{C_w m} = \frac{1.279 \text{ W} \times 1 \text{ s}}{4.2 \times 10^3 \text{ J/kg} \cdot ^\circ\text{C} \times 3.178 \text{ g}} = 0.0957^\circ\text{C}$$

where C_w is the specific heat capacity of water ($4.2 \times 10^3 \text{ J/kg} \cdot ^\circ\text{C}$).

The water temperature after 1s illumination is:

$$20 + 0.0957 = 20.0957^\circ\text{C}$$

For the next cycle, the same calculation procedure takes place, with a starting water temperature of 20.0957°C (293.2457 K).

$$p_{ws} = e^{(77.3450 + 0.0057 T - (7235 / T)) / T^{8.2}} = 2331.901 \text{ (Pa)} \quad p_a = 101.325 \text{ kPa}$$

$$x_s = 0.62198 p_{ws} / (p_a - p_{ws}) = 0.62198 p_{ws} / (101325 - p_{ws}) = 0.01465$$

$$g_s = (25 + 19v)A(1 - 60\%)x_s / 3600$$

$$= 6.71 \times 10^{-8} \text{ kg/s}$$

$$q = 2270 \text{ kJ/kg} \times 6.71 \times 10^{-8} \text{ kg/s}$$

$$= 0.152 \text{ J/s}$$

$$= 0.152 \text{ W}$$

$$q_e = P - q = 1.43 - 0.152 = 1.278 \text{ W}$$

The instantaneous water evaporation rate and light to evaporation conversion efficiency are calculated as:

$$v = g_s \times 3600 \times 10000/A \quad (\text{S-9})$$

$$\eta = 2270 \times v \times 100/3600 \quad (\text{S-10})$$

where v is instantaneous evaporation rate ($\text{kg/m}^2\text{h}$), and η is light to evaporation conversion efficiency (%). This computing process continues until $q_e = Q - q - P = 0$, which means all the available energy is utilized fully and there is no extra energy for further water evaporation. In the model, the water temperature, water evaporation rate, and light to evaporation efficiency all reach their peak points and would level off beyond this point.

1. Z. Wang, Y. Liu, P. Tao, Q. Shen, N. Yi, F. Zhang, Q. Liu, C. Song, D. Zhang, W. Shang and T. Deng, *Small* 2014, 10, 3234-3239.
2. H. Ghasemi, G. Ni, A. M. Marconnet, J. Loomis, S. Yerci, N. Miljkovic and G. Chen, *Nat Commun* 2014, 5.
3. L. Zhang, B. Tang, J. Wu, R. Li and P. Wang, *Adv. Mater.* 2015, 27, 4889-4894.
4. Y. Ito, Y. Tanabe, J. Han, T. Fujita, K. Tanigaki and M. Chen, *Adv. Mater.* 2015, 27, 4302-4307.
5. Y. Liu, S. Yu, R. Feng, A. Bernard, Y. Liu, Y. Zhang, H. Duan, W. Shang, P. Tao, C. Song and T. Deng, *Adv. Mater.* 2015, 27, 2768-2774.
6. Y. Liu, J. Chen, D. Guo, M. Cao and L. Jiang, *ACS Appl. Mater. Interfaces* 2015, 7, 13645-13652.
7. L. Zhou, Y. Tan, J. Wang, W. Xu, Y. Yuan, W. Cai, S. Zhu and J. Zhu, *Nat Photon* 2016, 10, 393-398.
8. K. Bae, G. Kang, S. K. Cho, W. Park, K. Kim and W. J. Padilla, *Nat Commun* 2015, 6.

9. Y. Wang, L. Zhang and P. Wang, ACS Sustainable Chem. Eng 2016, 4, 1223-1230.
10. G. Ni, G. Li, S. V. Boriskina, H. Li, W. Y, T. Z and G. Chen, Nature Energy 2016, 1, 16126
11. X. Li, W. Xu, M. Tang, L. Zhou, B. Zhu, S. Zhu and J. Zhu, Doi: 10.1073/pnas.1613031113
12. V. Mishra, I. Naveen, S. Purkayastha, S. Gupta, International Journal of Advanced Research in Computer Science and Software Engineering 2013, 3, 300-305.
13. O. Vaisala, 2010.
14. M. E. Jensen, In Estimating evaporation from water surfaces, Proceedings of the CSU/ARS Evapotranspiration Workshop, 2010; pp 1-27.
15. W. C. Turner, S. Doty, Energy management handbook. The Fairmont Press, Inc.: 2007.
16. F. Porges, Handbook of heating, ventilating and air conditioning. Butterworth-Heinemann: 2013.